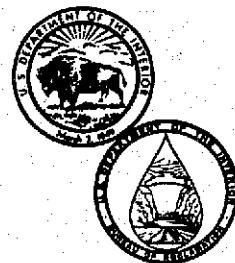


REC-ERC-79-6

SHAFT TORSIONAL OSCILLATIONS OF HYDROGENERATORS

**Engineering and Research Center
Bureau of Reclamation**

August 1979



TECHNICAL REPORT STANDARD TITLE PAGE

| | | | | | |
|--|--|-----------------------------|--|---|--|
| 1. REPORT NO. REC-ERC-79-6 | | 2. GOVERNMENT ACCESSION NO. | | 3. RECIPIENT'S CATALOG NO. | |
| 4. TITLE AND SUBTITLE Shaft Torsional Oscillations of Hydrogenerators | | | | 5. REPORT DATE August 1979 | |
| | | | | 6. PERFORMING ORGANIZATION CODE | |
| 7. AUTHOR(S) L. E. Ellits and Eugene Campbell | | | | 8. PERFORMING ORGANIZATION REPORT NO. REC-ERC-79-6 | |
| 9. PERFORMING ORGANIZATION NAME AND ADDRESS Bureau of Reclamation Engineering and Research Center Denver, Colorado 80225 | | | | 10. WORK UNIT NO. | |
| | | | | 11. CONTRACT OR GRANT NO. | |
| 12. SPONSORING AGENCY NAME AND ADDRESS Same | | | | 13. TYPE OF REPORT AND PERIOD COVERED | |
| | | | | 14. SPONSORING AGENCY CODE | |
| 15. SUPPLEMENTARY NOTES | | | | | |
| 16. ABSTRACT <p>This report describes efforts to analyze, model, and instrument the shaft torsional oscillations of electric generators. The mechanics of the shaft torsional modes are presented through the defining analytical equations from which block diagram and analog computer representation of shaft torsional systems have been developed. Results of an analog study of the torsional mode of a hydrogenerator as well as calculated data for several Bureau of Reclamation hydrogenerators are presented. An instrumentation system which employs shaft-mounted strain gages to provide a torsional signal has been developed for direct field measurement of the torsional behavior of hydrogenerator shafts. The design and circuit configuration of that instrumentation system are presented. Results from field measurements of the shaft torsional oscillations at three sites are also presented.</p> | | | | | |
| 17. KEY WORDS AND DOCUMENT ANALYSIS | | | | | |
| a. DESCRIPTORS-- / analog computers/ electric generators/ *elasticity (mechanical)/ dynamic response/ instrumentation/ mechanics/ natural frequency/ *prototype tests/ hydroelectric powerplants/ resonance/ rotating components/ *strain gages/ stiffness/ *torsion/ vibration damping/ | | | | | |
| b. IDENTIFIERS-- / Flatiron Powerplant, CO/ Grand Coulee Powerplant, WA/ Southern Nevada Water Project, NV/ | | | | | |
| c. COSATI Field/Group 09C COWRR: 09 03 | | | | | |
| 18. DISTRIBUTION STATEMENT Available from the National Technical Information Service, Operations Division, Springfield, Virginia 22161. | | | | 19. SECURITY CLASS (THIS REPORT) UNCLASSIFIED | |
| | | | | 21. NO. OF PAGES 25 | |
| | | | | 20. SECURITY CLASS (THIS PAGE) UNCLASSIFIED | |
| | | | | 22. PRICE | |

REC-ERC-79-6

**SHAFT TORSIONAL OSCILLATIONS
OF HYDROGENERATORS**

by

L. E. Eilts

Eugene Campbell

August 1979

Electric Power Branch
Division of Research
Engineering and Research Center
Denver, Colorado



UNITED STATES DEPARTMENT OF THE INTERIOR

* BUREAU OF RECLAMATION

REC-ERC-79-6

**SHAFT TORSIONAL OSCILLATIONS
OF HYDROGENERATORS**

by

L. E. Eilts

Eugene Campbell

August 1979

Electric Power Branch
Division of Research
Engineering and Research Center
Denver, Colorado



UNITED STATES DEPARTMENT OF THE INTERIOR

★ BUREAU OF RECLAMATION

ACKNOWLEDGMENTS

The laboratory research investigations and field tests of shaft torsional oscillations included in this report and the design and development of the torsional instrumentation system were performed by personnel of the Electric Power Branch under the supervision of Charles L. Clemans.

Richard C. Arbour, Head, Laboratory and Special Projects Section, and Richard J. Brown of the Dams Branch, Division of Design, participated in the field tests conducted at the Southern Nevada Water Project pumping plants in January 1978.

The authors are indebted to regional and project personnel for the opportunity to conduct developmental field testing of the torsional instrumentation systems at Flatiron and Grand Coulee Powerplants and at the Southern Nevada Water Project pumping plants.

CONTENTS

| | Page |
|--|------|
| Letter symbols and quantities | iii |
| Purpose | 1 |
| Conclusions | 1 |
| Applications | 1 |
| Introduction | 1 |
| Mechanics of shaft torsional oscillations | 2 |
| Torsional oscillations of a hydrogenerator shaft | 2 |
| Analog modelling | 2 |
| Field experience | 6 |
| Shaft torsional instrumentation system | 7 |
| General description | 7 |
| Circuit description | 9 |
| Appendix A | 19 |
| Appendix B | 25 |

TABLE AND FIGURES

Table

| | | |
|---|---------------------------------------|-----|
| I | Calculated shaft torsional data | 8,9 |
|---|---------------------------------------|-----|

Figure

| | | |
|----|--|----|
| 1 | General torsional spring-mass system | 3 |
| 2 | Simplified diagram of the torsional system of a vertical waterwheel generator | 4 |
| 3 | Analog diagram for shaft torsional oscillations of a hydrogenerator | 5 |
| 4 | Torsional response of the analog system | 7 |
| 5 | Shaft torsional instrumentation system applied to Unit 1 at Flatiron Powerplant | 10 |
| 6 | Torsional oscillation of Unit 1 at Flatiron Powerplant | 10 |
| 7 | Shaft torsional instrumentation system applied to Unit G19 at Grand Coulee | 10 |
| 8 | Torsional oscillation excited by a 600-MW load rejection from Unit G19 at Grand Coulee | 11 |
| 9 | Modified shaft torque instrumentation system applied to Unit 6 of Pumping Plant No. 1 of the Southern Nevada Water Project | 12 |
| 10 | Shaft torsional oscillation of Unit 6 of Southern Nevada Water Project, Pumping Plant No. 1 | 12 |
| 11 | Block diagram of the shaft torsional instrumentation system | 12 |
| 12 | Torque sensor and frequency-modulated transmitter schematic | 13 |
| 13 | Pulse receiver schematic | 14 |
| 14 | Demodulator schematic | 15 |
| 15 | Schematic diagrams of the active filters | 16 |
| A1 | Block diagram of the torsional system of figure 1 | 20 |

LETTER SYMBOLS AND QUANTITIES

| SYMBOL | QUANTITY | SYMBOL | QUANTITY |
|-------------|---|---------------------------|---|
| a | Tangential acceleration at the shaft surface | n_R | Rated speed in r/min (revolutions per minute) |
| D | Shaft outside diameter in inches | P_R | Generator rated power output in megawatts |
| D_i | Damping proportionality constant for internal damping of shaft section S_i | R | Damping proportionality constant of rotating mass |
| D_m | Damping proportionality constant for internal damping of the shaft connecting the turbine runner to the generator rotor | R_e | Damping proportionality constant of the generator rotor |
| D_{norm} | Total normalized damping, including turbine runner, generator, and internal shaft damping | R_i | $i = 1, 2, 3, \dots$ Damping proportionality constant of the i th rotating mass |
| d | Shaft outside diameter in meters | R_j | Damping proportionality constant of the turbine runner |
| d/dt | Time derivative | S_{ij} | Shaft section connecting mass i to mass j |
| e | Naperian logarithm base | ΔS | Shaft surface deflection per unit length at rated generator output power |
| f | Damped torsional oscillation frequency in hertz | s | La Place operator |
| f_n | Undamped natural oscillation frequency in hertz | Δs | Shaft surface deflection per unit length due to torsional oscillation |
| g | Gravitational constant (acceleration) | T_m | Mechanical starting time |
| Hz | Cycles per second in hertz | T_{m_e} | Mechanical starting time of the generator rotor |
| h | Damping factor | T_{m_i} | $i = 1, 2, 3, \dots$ Mechanical starting time of the i th rotating mass |
| hp | Horsepower | T_{m_r} | Mechanical starting time of the turbine runner |
| I | Moment of inertia in kg·m | t | Time |
| I_i | $i = 1, 2, 3, \dots$ Moment of inertia i th rotating mass in kg·m | WR^2 | Moment of inertia in lb·ft ² |
| K | Shaft torsional spring constant | $(WR^2)_i$ | Moment of inertia of the i th mass in lb·ft ² |
| K_n | Shaft torsional spring constant of shaft section S_n | X_c | Capacitive reactance |
| K_{m_n} | Per unit shaft torsional spring constant | X_L | Inductive reactance |
| K_{s_n} | Synchronizing coefficient of the swing equation in per unit torque per electrical degree | α_e | Angular acceleration of the generator rotor |
| L | Overall shaft length in inches | α_i | Angular acceleration of the turbine runner |
| l | Overall shaft length in meters | ζ | Synchronous machine internal torque angle |
| M | Moment or torque | η_e | Generator efficiency |
| M_R | Rated moment or torque | Θ_n | Constant angular shaft deflection for rated generator output |
| M_e | Generator rotor airgap torque | Θ_e | Constant angular deflection of the generator rotor |
| M_i | $i = 1, 2, 3, \dots$ Moment or torque applied to the i th rotating mass | Θ_i | $i = 1, 2, 3, \dots$ Constant angular deflection of the i th mass |
| M_r | Turbine runner mechanical input torque | Θ_j | Constant angular deflection of the j th mass |
| ΔM | Torque disturbance | Θ_r | Constant angular deflection of the turbine runner |
| m | Per unit torque | $(\Theta_i - \Theta_e)IC$ | Initial condition of angular displacement difference (Note: All above angles (Θ) are measured with respect to a synchronously rotating reference frame.) |
| M_i | Per unit torque applied to the i th rotating mass | | |
| m_{ij} | Torque transmitted from the i th mass to the j th mass by the shaft section S_{ij} | | |
| $m_{i,i}$ | Per unit reaction torque on the i th mass in response to torques transmitted by the shaft from the $(i-1)$ th mass | | |
| $m_{i,i+1}$ | Per unit reaction torque on the i th mass in response to torques transmitted by the shaft from the $(i+1)$ th mass | | |

LETTER SYMBOLS AND QUANTITIES — Continued

| | |
|---------------|---|
| π | 3.141 59. . . |
| Σ | Summation |
| σ | Logarithmic decrement factor |
| ω_0 | Initial condition of the angular velocity |
| ω_2 | Angular velocity of the generator rotor |
| ω_i | $i = 1, 2, 3, \dots$ Angular velocity of the i th rotating mass |
| ω_j | $j = 1, 2, 3, \dots$ Angular velocity of the j th rotating mass |
| ω_n | $n = 1, 2, 3, \dots$ Angular velocity of the n th device. |
| ω_R | Rated angular velocity |
| ω_{0T} | Initial condition of the angular velocity of the turbine runner |
| ω_T | Angular velocity of the turbine runner |
| Ω | Ohms |
| k Ω | Thousand ohms |
| MW | Megawatt |
| mA | Milliamper |
| mils | Length equal to 1/1000 inch |
| pF | Picofarad or 10^{-12} farad |
| μ F | Microfarad or 10^{-6} farad |
| V | Volt |

PURPOSE

The purposes of the research reported here were to analyze, model, and instrument the torsional oscillations of hydrogenerator shafts to gain additional insight into the torsional behavior of hydrogenerators and to assess the influence of modern high-initial-response static excitation systems upon the damping of the torsional oscillations.

CONCLUSIONS

1. Shaft torsional phenomena have been modeled by appropriate mathematical equations from which block diagram and analog computer models have been developed.
2. Hydrogenerators are generally characterized by a single shaft torsional mode of oscillation which is adequately damped due to viscous waterwheel damping.
3. The large inertia of hydrogenerator rotors very effectively limits the influence of the electrical system upon the mechanical shaft torsional vibrations. Consequently, it is relatively difficult to excite shaft torsional oscillations by disturbances applied to the generator. Moreover, generator damping is generally ineffective in damping the torsional oscillations of the shaft because of the large generator inertia. As a result, a hydrogenerator excitation system generally has negligible influence upon the shaft torsional oscillations.
4. An instrumentation system for prototype field measurement of shaft torsional behavior has been developed and utilized to obtain shaft torsional data from several units.

APPLICATIONS

The information presented in this report is specifically applicable to hydrogenerators. However, most of the results are equally applicable to other types of generators providing suitable consideration is given to inherent design differences. The tests at Grand Coulee Powerplant demonstrate the limited influence which the excitation system may exert upon the shaft torsional oscillations. Consequently, the investigators plan no additional work on shaft torsional oscillations. However, the instrumentation system may be further applied in measuring steady-state shaft torque (turbine output).

INTRODUCTION

In recent years much interest has been focused on the natural torsional oscillations within the shafts of synchronous machines. There are two basic phenomena which have spurred this interest:

1. The practice of employing series-capacitor compensation to extend the stability limits of long EHV (extra-high voltage) transmission lines radiating from large generating stations can introduce subsynchronous currents (of frequency $60 \sqrt{X_c/X_l}$) on the transmission lines. As a result the generator experiences pulsating torques at frequencies equal to the sum and difference of normal system frequency (60 Hz) and the subsynchronous frequency. Should the frequency of these pulsating torques lie close to a natural mechanical torsional frequency of the shaft, dangerously severe stresses may occur in the shaft and ultimately lead to its failure. Although the sum frequency is well removed from the torsional frequencies, the difference frequency may indeed lie close to a torsional frequency.

2. The natural shaft torsional frequencies are generally very lightly damped; hydrogenerators are, however, usually better damped than steam-driven machines. The recent availability of high voltage power thyristors has led to control systems such as HVDC (high voltage direct-current) converters and HIR (high-initial-response) excitation systems which are sufficiently potent and responsive as to influence shaft torsional oscillations. The broad band capability of these static control systems has made it possible to excite the torsional modes of the shaft through normal control action. Although the Bureau of Reclamation has no HVDC transmission facilities, several HIR excitation systems have been acquired in recent years. Such excitation systems — particularly when equipped with PSS (power system stabilizers) — may indeed excite or aggravate the natural torsional modes resulting in undue shaft stresses.

To assess the influence upon the natural torsional modes of the shaft from either of these sources, it is first necessary to understand the physics of the torsional vibrations. This report describes efforts to analyze, model, and instrument shaft torsional oscillations in order to assess the influence of modern HIR excitation systems equipped with PSS upon the torsional oscillations of hydrogenerator shafts. However, most of the results are equally applicable to other types of generators.

MECHANICS OF SHAFT TORSIONAL OSCILLATIONS

The shaft of a synchronous generator generally connects several rotating masses, including the generator rotor, turbine rotors, and sometimes the rotor of a rotating exciter as illustrated in figure 1. Each section S_n of the shaft has a characteristic torsional spring constant K_n and some inherent damping D_n . In addition, the rotating masses generally contribute their own damping R , due to losses such as friction, windage, viscous damping, and frequency-dependent electrical loads on the generator. The resulting system constitutes a coupled, torsional, spring-mass system which is characterized by n nodes of oscillation, where n is the number of shaft sections. The equations appropriate for describing the system of figure 1 are developed in appendix A and a block diagram representation of this system is presented in figure A1. The system of figure 1 is typical of steam driven alternators where there generally are several cascaded steam turbines and, therefore, several characteristic modes of oscillation. Fortunately, most hydrogenerators have only one turbine runner (the waterwheel), a generator rotor, and possibly a rotating exciter. The hydrogenerators of particular concern are those with HIR excitation systems which are often not shaft mounted. These systems thus possess only two rotating masses — that of the turbine runner and the generator rotor. Therefore, the remainder of this report shall concern only two mass systems. It should be noted, however, that the addition of a rotating exciter will merely serve to introduce an additional mode of oscillation (between the generator and exciter rotors) which is essentially independent of the oscillation between the generator rotor and the turbine runner.

TORSIONAL OSCILLATIONS OF A HYDROGENERATOR SHAFT

Analog Modelling

As pointed out in the preceding section, hydrogenerators typically exhibit a single principal mode of torsional oscillation. A simplified diagram of the turbine runner-shaft-generator rotor system of a vertical waterwheel generator is presented in figure 2. This system may be described as in appendix A by equations 4a, 4b, and 8a. From those equations, the analog computer model of figure 3 was developed to investigate the torsional mode of oscillation and to provide insight into the torsional phenomena.

Generally, the mechanical starting times of the generator rotor T_{m_g} and of the turbine runner T_{m_r} as

well as the torsional spring constant K_m of the shaft, may be determined analytically for inclusion in the analog model. The damping coefficients (turbine runner damping R_r , generator damping R_g , and internal shaft damping D_{ie}) are, however, seldom accurately known and must be estimated. Realistic practical values for R_r and R_g have been taken as 2.5 and 1.0, respectively, in stability studies and excitation and governing system studies. To reasonably represent the modest internal damping of the shaft steel, a damping coefficient of approximately 5 percent of that corresponding to critical damping may be used.

An analog study of the torsional mode of a 108-MW unit in the Grand Coulee Powerplant was conducted using the model and constants shown in figure 3. Digital analysis of the characteristic equation of this system revealed that the damping factor ζ used in the study was actually 0.044, consequently oscillations diminish to 10 percent in 8.3 cycles.

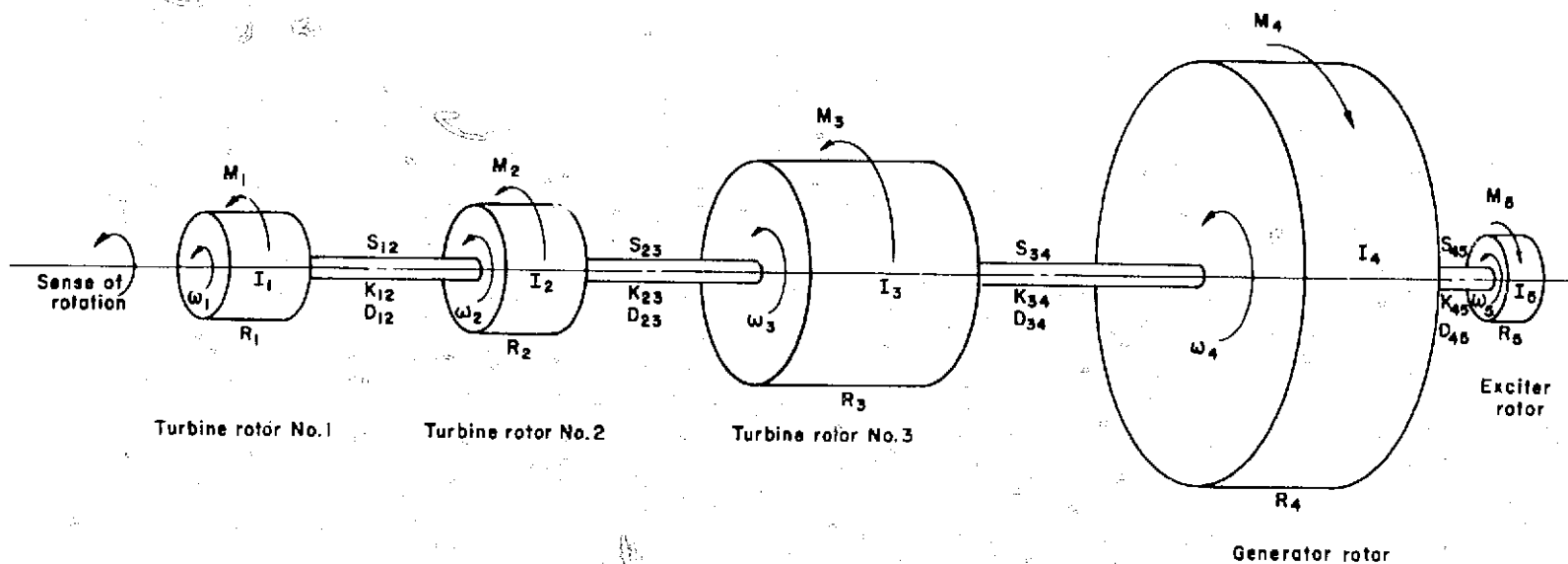
Several interesting conclusions from that study are presented in the following. Analytical relations pertinent to the torsional behavior of a hydrogenerator are presented in appendix B.

For typical damping coefficients, the observed damped torsional frequency $f = f_n \sqrt{1 - \zeta^2}$ differs very little from the natural frequency f_n which, as presented in appendix B, depends only upon the turbine runner and generator rotor inertias and the torsional spring constant of the shaft.

An expression for the relative damping influences in the analog system of figure 3 is given by:

$$D_{total} (T_{m_g} + T_{m_r}) = T_{m_g} R_g + T_{m_r} R_r + D_{ie} (T_{m_r} + T_{m_g})$$

Because of the distribution of the inertia in a hydrogenerator it is readily concluded that generator damping R_g will be much less influential in damping shaft torsional oscillations than either waterwheel damping R_r or internal shaft damping D_{ie} . This was indeed substantiated by the study. Generator damping has an insignificant influence on the decrement of the shaft torsional oscillations because the large mass of the generator rotor prevents it from responding with the shaft oscillations. In the study, increasing R_g from zero to 50 resulted in only a 4-percent increase in the damping rate. Turbine runner damping was, however, quite effective in damping the shaft torsional oscillations. For example, as turbine runner damping R_r was increased from zero to 10 in the analog study, the damping rate increased more than six-fold (ζ increased from 0.044 to 0.282). Use of the realistic hydraulic turbine self-regulation (or damping) coefficient of 1.0 suggested in a preceding



- S_{ij} - Shaft section connecting the i th and j th rotating masses.
 M_i - Moment or torque applied to the i th rotating mass.
 ω_i - Angular velocity of the i th rotating mass.
 I_i - Moment of inertia of the i th rotating mass.
 K_{ij} - Torsional spring constant of the shaft section S_{ij} .
 D_{ij} - Damping proportionality constant for the internal damping of shaft section S_{ij} .
 R_i - Damping proportionality constant for the i th rotating mass.

Figure 1. - General torsional spring-mass system.

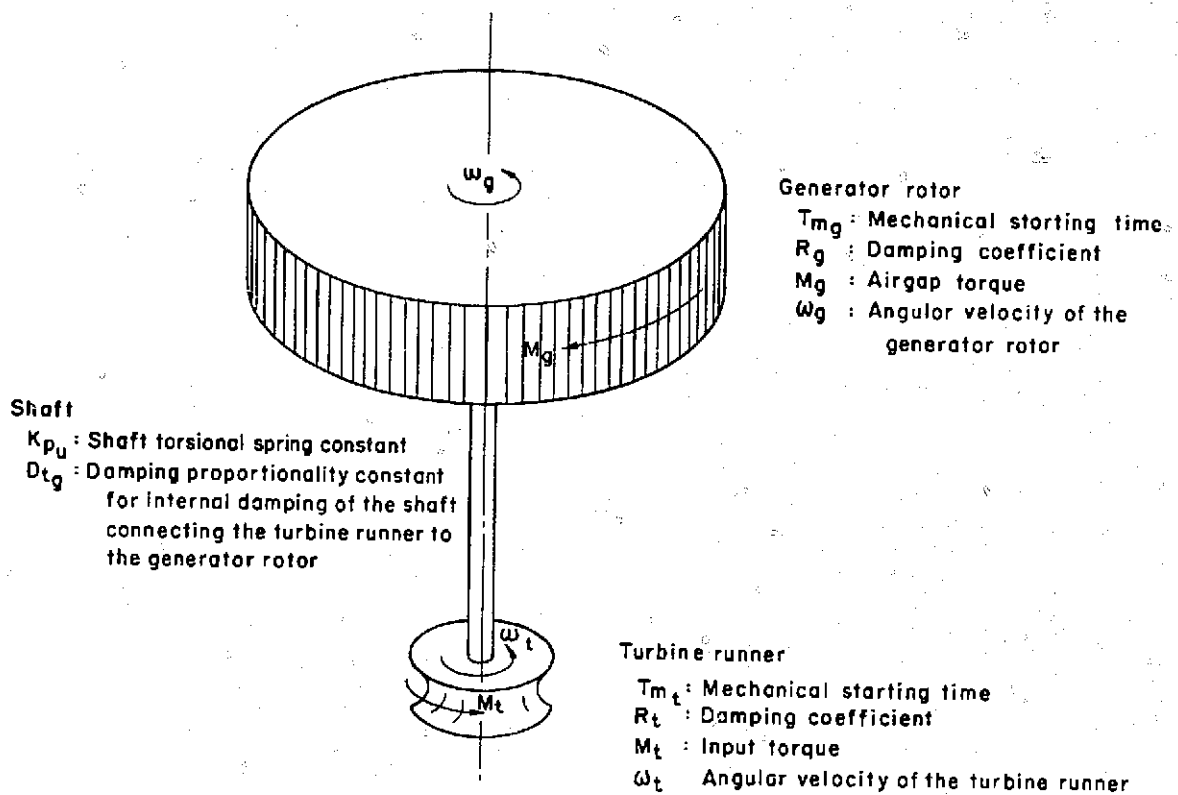
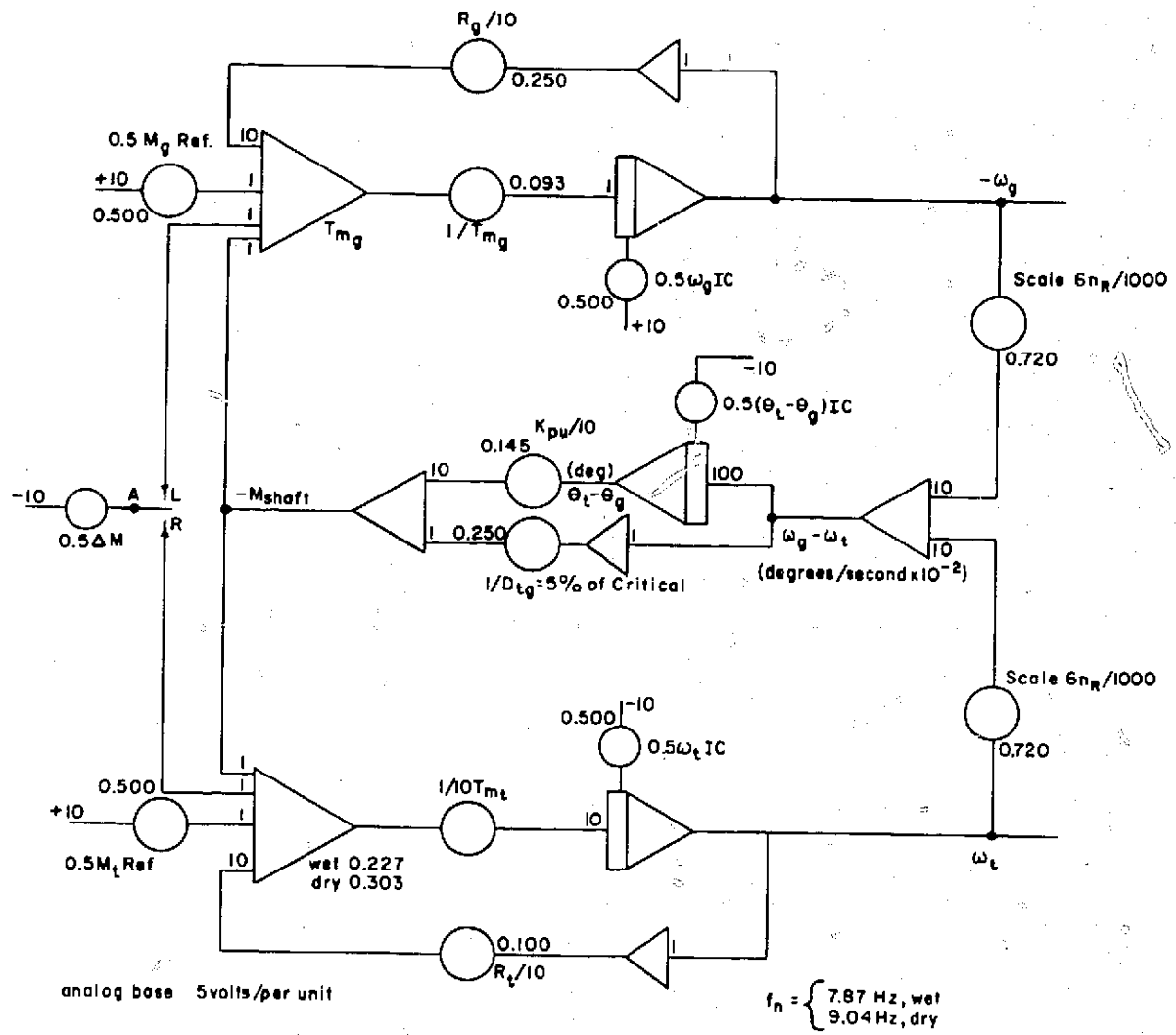


Figure 2.—Simplified diagram of the torsional system of a vertical waterwheel generator.



Note: The potentiometer settings shown on this diagram are those used in a study of the IOBMW units of the Grand Coulee Powerplant.

Figure 3. - Analog diagram for shaft torsional oscillations of a hydrogenerator.

paragraph increased the damping rate approximately 50 percent ($\zeta = 0.066$) over that obtained with no turbine runner damping. It is noted that steam-driven generators are characterized by little or no turbine impeller damping which contributes to their acute torsional problems.

The amplitude of the shaft torsional mode excited by a specific torque disturbance is shown in appendix B to be similarly related to the distribution of the system inertia. That is, a one per unit torque input via the waterwheel couples energy into the shaft torsional mode much more effectively than a one per unit torque input from the generator; in fact, the torsional amplitudes are related inversely as the inertias. Consequently, electrical disturbances to the generator (such as faults, load rejections, out-of-step synchronizing, etc.) stress the shaft much less severely than hydraulic disturbances (such as draft tube, penstock, or waterhammer surges) of similar amplitude. The large generator inertia very effectively attenuates disturbances applied to the shaft across the air gap of the generator. A sample shaft torsional response from the analog study is presented in figure 4. The observed frequency of oscillation compares well with analytical predictions.

The shaft torsional frequencies of hydrogenerators generally lie in the range 5 to 15 Hz although somewhat higher frequencies of oscillation may be observed for high-speed units. Table 1 summarizes calculated data related to the torsional modes of several Bureau of Reclamation hydrogenerators. It is particularly interesting to note that even though the ratings of the units listed in the table vary widely, the per unit shaft torsional spring constant K_{θ} only varies from 1.2 to 2.7 per unit per mechanical degree. Field measurements have been made on some of the units listed and are discussed in table 1.

Field experience

To assess the rate at which the torsional oscillations of a hydrogenerator are damped, and more specifically, to assure that the damping rate is not diminished by excitation control, an effort was made to develop instrumentation suitable for recording the torsional oscillations of the shaft. Three possible signal sources were considered: differential speed measured across the shaft, tangential acceleration at the surface of the shaft, and mechanical strain of the shaft. The differential quality needed to extract the small torsional component of speed from the output of available speed transducers made that scheme unattractive. Transducers (accelerometers) suitable for recording the shaft torsional oscillations by measuring tangential acceleration were available,

but the instrumentation (particularly the charge amplifier) commonly applied to convert the accelerometer output to a useful signal was less attractive than that used in the other schemes.

Consequently, mechanical shaft strain, as measured by strain gages attached to the rotating shaft, was selected as the signal source for recording torsional oscillations of the shaft.

In May 1975, an instrumentation system that had been developed in the laboratory was initially field tested on unit 1 at Flatiron Powerplant (fig. 5). Those preliminary tests demonstrated both the feasibility of the instrumentation technique and the suitability of the strain signal for recording shaft torsional oscillations. The torsional oscillation of figure 6 resulted from the very small electrical disturbance which occurred when the unit was tripped from the line during a normal shutdown sequence by the operator. The measured shaft strain is accordingly quite small, but sufficient to determine the natural frequency of oscillation and the damping factor. Both the natural frequency of oscillation and the damping rate are higher than generally expected, presumably because of the relatively high speed of the Flatiron unit (514 r/min).

With only minor scaling modifications, the same instrumentation system was used at Grand Coulee in September 1975 to record the torsional oscillations of the shaft of generating unit G19 in the Third Powerplant (fig. 7). The torsional oscillations recorded during a 600 MW load rejection test are presented in figure 8. A particularly interesting observation from that test concerns an increase noted in the natural frequency of oscillation after the wicket gates have closed and as the draft tube pulls a vacuum, effectively unwatering the turbine. The observed rise in frequency is similar to that of the "wet" and "dry" turbines in table 1. The natural frequency and damping rate of the torsional oscillations shown in figure 8 are more typical of a hydrogenerator than those of figure 6 as explained above. Tests on unit G19 at Grand Coulee verified that the influence of excitation control upon the shaft torsional oscillations is indeed negligible due to the huge inertia of the generator rotor. Excitation control generally neither improves nor diminishes the damping of shaft torsional oscillations of hydrogenerators. Unit G19 tests also verified that the shaft torsional mode is excited much easier from the turbine than from the generator — hydraulic disturbances continually excite the shaft mode. Specifically, it was observed that the strongest shaft torsional oscillations were excited during breakaway, when a substantial (possibly 10 to 25 percent) torque is quickly applied directly to the turbine.

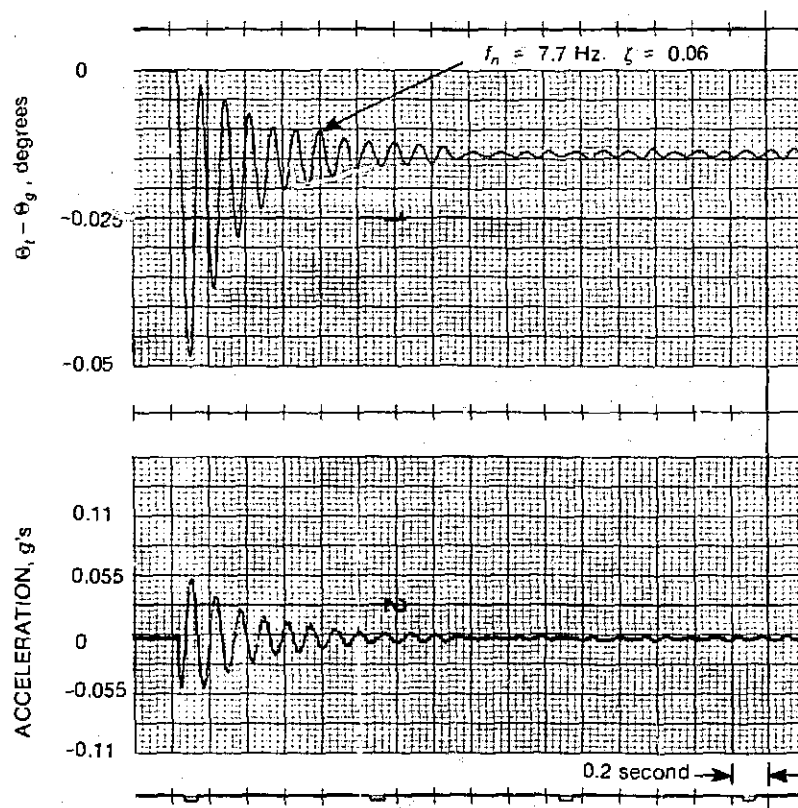


Figure 4.—Torsional response of the analog system (1.0 per unit disturbance applied to the generator, $R_t = 1.0$, $R_g = 2.5$).

In an effort to evaluate the performance of several pumps in the Southern Nevada Water Project system, simultaneous recordings of electrical power, shaft torque, speed, and hydraulic pressure were desired. Of these signals, only shaft torque was not readily available, although it was suspected that the shaft torsional instrumentation system might be adapted to provide that signal. To accomplish the measurement of pump shaft torque, the torsional instrumentation system had to be modified to provide steady-state absolute torque rather than merely torque deviations and the physical size of the rotating portion of the measurement system had to be markedly reduced to fit it on the small exposed portion of the pump shaft. The resulting instrumentation system shown in figure 9 was applied at the pumping plants in January 1978. Figure 10 is a record of the torsional oscillation which resulted when the pump was started. The recorded oscillation was obtained by differentiating the steady-state torque signal. Because the shaft of the particular pump examined (fig. 10) is unusually long and slender, the torsional spring constant is accordingly rather

small resulting in unusually large torsional amplitudes and a rather low natural torsional frequency for such a high-speed unit (900 r/min).

The modified instrumentation system suitable for steady-state torque or torsional measurements is schematically presented and described in the following section.

SHAFT TORSIONAL INSTRUMENTATION SYSTEM

General Description

The instrumentation system is functionally divided into two main parts (fig. 11). One portion is attached to the shaft and rotates with it, while the other remains stationary. The portion of the system on the shaft consists of a strain gage bridge incorporating four active gages oriented to sense torsional strain in the shaft, an instrumentation-type difference amplifier, an FM (frequency-modulated) pulse

Table I.—Calculated shaft torsional data — metric units

| Term | Glen Canyon G1 - G8 | Flatiron 1 and 2 | Grand Coulee G19, G20, G21 | Grand Coulee | G1 - G18 | Grand Coulee P G7 & P G8 | |
|--|--------------------------------------|---------------------|-------------------------------|--------------|----------|-----------------------------|-------|
| Generator Rated output | MW | 112.5 | 35 | 600 | 108 | (125) [†] | 50 |
| Rated speed | r/min | 150 | 514 | 72 | 120 | | 200 |
| Turbine rated power* | MW | 115 | 35.8 | 618.9 | 111.1 | 129 | 50.7 |
| Shaft nominal outside diameter | mm | 1016 | 483 | 2540 | 1118 | | 686 |
| Shaft nominal inside diameter | mm | 203 | 102 | 2134 | 305 | | 160 |
| Torsional spring constant | (N·m/rad) 10 ⁹ | 0.895 | 0.079 | 12.089 | 0.712 | | 0.208 |
| Normalized torsional spring constant | per unit/deg | 2.181 | 2.120 | 2.652 | 1.45 | (1.25) | 1.52 |
| Generator WR^2 | (kg·m ²) 10 ⁶ | 3.034 | 0.075 | 107.0 | 7.332 | | 0.653 |
| Turbine WR^2 | (kg·m ²) 10 ³ | 196.8 | 5.900 | 8428 | 303 | | 90.60 |
| Turbine WR^2 — dry | (kg·m ²) 10 ³ | 141.2 | 3.961 | 5562 | 227 | | 60.68 |
| Generator mechanical starting time | s | 6.65 | 6.25 | 10.14 | 10.72 | (9.26) | 5.73 |
| Turbine mechanical starting time — dry | s | 0.31 | 0.33 | 0.53 | 0.33 | (0.29) | 0.53 |
| Turbine mechanical starting time | s | 0.43 | 0.49 | 0.80 | 0.44 | (0.38) | 0.79 |
| Natural torsional frequency — dry | Hz | 12.96 | 23.06 | 7.61 | 9.04 | | 9.74 |
| Natural torsional frequency | Hz | 11.08 | 19.12 | 6.26 | 7.87 | | 8.14 |
| Rated moment (torque) | (N·m) 10 ⁶ | 7.16 | 0.65 | 79.59 | 8.60 | (9.95) | 2.39 |
| Angular shaft deflection at rated output | degree | 0.46 | 0.47 | 0.38 | 0.69 | (0.80) | 0.66 |
| Total shaft surface deflection at rated output | mm | 4.191 | 1.981 | 8.357 | 6.756 | (7.798) | 3.937 |
| Peak angular shaft torsional deflection: | | | | | | | |
| From 1 per unit generator torque | degree | 0.028 | 0.034 | 0.028 | 0.027 | (0.032) | 0.08 |
| From 1 per unit turbine torque | degree | 0.43 | 0.44 | 0.35 | 0.66 | (0.77) | 0.58 |
| Peak total shaft torsional surface deflection: | | | | | | | |
| From 1 per unit generator torque | mm | 0.249 | 0.144 | 0.610 | 0.269 | (0.310) | 0.480 |
| From 1 per unit turbine torque | mm | 3.813 | 1.844 | 7.747 | 6.477 | (7.493) | 3.454 |

[†] Rerated constants shown in parentheses.

* Assuming a generator efficiency of 0.97.

** Unless specifically indicated as dry, all data are given for a watered turbine with the mass of the water included with the mass of the turbine.

generator, and a transmitter coil. The difference amplifier serves to amplify the bridge unbalance due to torsion and provides the voltage signal used to modulate the frequency of the pulse generator via a VCO (voltage controlled oscillator). The pulse generator output is delivered to the primary of a coupling transformer (coil) made up of a few turns of insulated wire wound around the shaft and rotating with it. The stationary part of the system, which begins at the secondary of the transformer and is necessarily located in close proximity to the shaft, is comprised of a pulse receiver, an FM demodulator, an output amplifier, and signal filters. Both high- and low-pass filters are available to bracket the expected frequency range of the analog signal. The filters are not always necessary.

To avoid the signal noise and sliding contact problems commonly associated with the use of slip rings in strain gage bridge circuits, an alternative method using transformer coupling for transmitting the

signal from the shaft to the stationary recording device was selected. To obtain a relatively long battery life (i.e., more than 24 hours of continuous operation) from a suitably small battery pack required unusually low bridge currents. The system designed has operated satisfactorily with a bridge current as low as 4 milliamperes (30 to 35 mA is common in conventional strain gage bridges).

The low duty cycle (less than 1 percent) allows relatively large amplitude current pulses to be circulated in the coupling transformer while maintaining low battery drain. Variations in amplitude of the coupled pulses — as the primary of the coupling transformer rotates — are inconsequential because the information is carried in the frequency of the coupled pulses rather than their amplitude. The symmetry of the bridge circuit and the high common-mode rejection of the difference amplifier provide sufficient stability that adequate sensitivity to reliably detect torsional oscillations may be realized.

Table 1.—Calculated shaft torsional data — U.S. customary units

| Term | Glen Canyon G1 - G8 | Flatiron 1 and 2 | Grand Coulee G19, G20, G21 | Grand Coulee | G1 - G18 | Grand Coulee P G7 & P G8 |
|--|--|---------------------|-------------------------------|--------------|--------------------|-----------------------------|
| Generator Rated output | MW 112.5 | 35 | 600 | 108 | (125) ⁺ | 50 |
| Rated speed | r/min 150 | 514 | 72 | 120 | | 200 |
| Turbine rated power* | hp 10 ³ 155 | 48 | 830 | 149 | (173) | 69 |
| Shaft nominal outside diameter | in 40 | 19 | 100 | 44 | | 27 |
| Shaft nominal inside diameter | in 8 | 4 | 84 | 12 | | 6.3 |
| Torsional spring constant | (lb-in/rad) 10 ⁹ 7.92 | 0.699 | 107 | 6.3 | | 1.84 |
| Normalized torsional spring constant | per unit/deg 2.181 | 2.120 | 2.652 | 1.45 | (1.25) | 1.52 |
| Generator WR^2 | (lb-ft ²) 10 ⁶ 72.0 | 1.79 | 2540 | 174 | | 15.5 |
| Turbine WR^2 | (lb-ft ²) 10 ⁶ 4.67 | 0.14 | 200 | 7.2 | | 2.15 |
| Turbine WR^2 — dry** | (lb-ft ²) 10 ⁶ 3.35 | 0.094 | 132 | 5.4 | | 1.44 |
| Generator mechanical starting time | s 6.65 | 6.25 | 10.14 | 10.72 | (9.26) | 5.73 |
| Turbine mechanical starting time — dry | s 0.31 | 0.33 | 0.53 | 0.33 | (0.29) | 0.53 |
| Turbine mechanical starting time | s 0.43 | 0.49 | 0.80 | 0.44 | (0.38) | 0.79 |
| Natural torsional frequency — dry | Hz 12.96 | 23.06 | 7.61 | 9.04 | | 9.74 |
| Natural torsional frequency | Hz 11.08 | 19.12 | 6.26 | 7.87 | | 8.14 |
| Rated moment (torque) | (lb-ft) 10 ⁶ 5.28 | 0.48 | 58.7 | 6.34 | (7.34) | 1.76 |
| Angular shaft deflection at rated output | degree 0.46 | 0.47 | 0.38 | 0.69 | (0.80) | 0.66 |
| Total shaft surface deflection at rated output | mils 165 | 78 | 329 | 266 | (307) | 155 |
| Peak angular shaft torsional deflection: | | | | | | |
| From 1 per unit generator torque | degree 0.028 | 0.034 | 0.028 | 0.027 | (0.032) | 0.08 |
| From 1 per unit turbine torque | degree 0.43 | 0.44 | 0.35 | 0.66 | (0.77) | 0.58 |
| Peak total shaft torsional surface deflection: | | | | | | |
| From 1 per unit generator torque | mils 9.8 | 5.67 | 24.0 | 10.6 | (12.2) | 18.9 |
| From 1 per unit turbine torque | mils 150.1 | 72.6 | 305 | 255 | (295) | 136 |

⁺ Rated constants shown in parentheses.

* Assuming a generator efficiency of 0.97.

** Unless specifically indicated as dry, all data are given for a watered turbine with the mass of the water included with the mass of the turbine.

Circuit Description

Strain gage bridge, amplifier, and pulse generator.—

The circuit configuration shown in figure 12 follows common practice; however, the use of integrated circuits together with a very low duty cycle pulse generator allows a small package with low battery drain (around 20 to 25 mA, total).

The bridge amplifier (Device 521) operates with a gain of 1000 and provides the signal that modulates the frequency of the VCO (Device 566). The square wave output of the VCO is differentiated by the 47pF capacitor and the negative excursion of the differentiator output momentarily turns on the transistor pair. The output transistor discharges the 0.005 μ F capacitor through the primary of the coupling transformer. The oscillator operates at a nominal center frequency of 10 kHz with a modulation sensitivity of approximately 4.6 kHz/V.

Pulse receiver.—

The pulse receiver of figure 13 consists of the receiver coil (transformer secondary), a field effect transistor input amplifier (Q_1), and four additional discrete transistor stages in complimentary pairs. The output from the final transistor is a 10-kHz pulse signal which drives a 4518 CMOS digital divider. The divider output provides a symmetric frequency-modulated square wave at a nominal frequency of 5 kHz which is routed to the demodulator circuitry.

Demodulator.—

The demodulator of figure 14 is a frequency-to-voltage converter, commonly called a frequency transducer. The positive excursion of the 5-kHz square wave signal from the pulse receiver closes analog switch B (of Device 7510) connecting a negative reference voltage from the power supply to operational amplifier OA1 which is connected as an integrator.

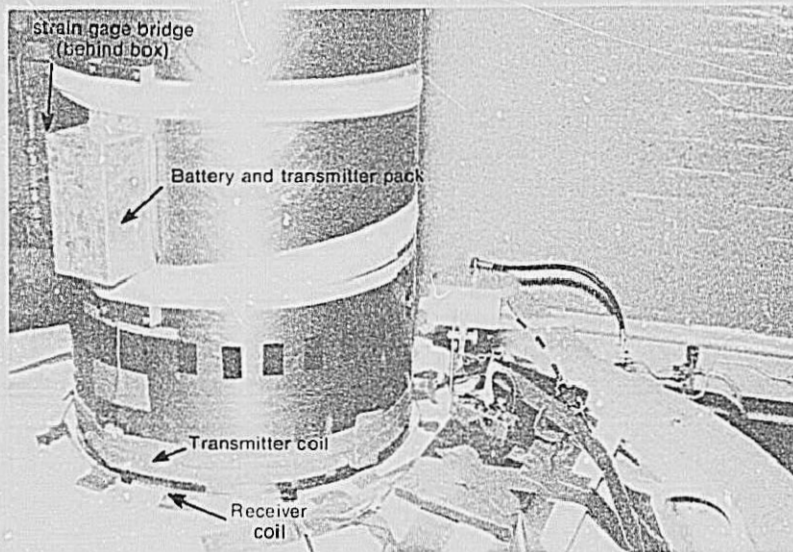


Figure 5.—Shaft torsional instrumentation system applied to Unit 1 at Flatiron Powerplant — May 1975. Photo C801-D-79091

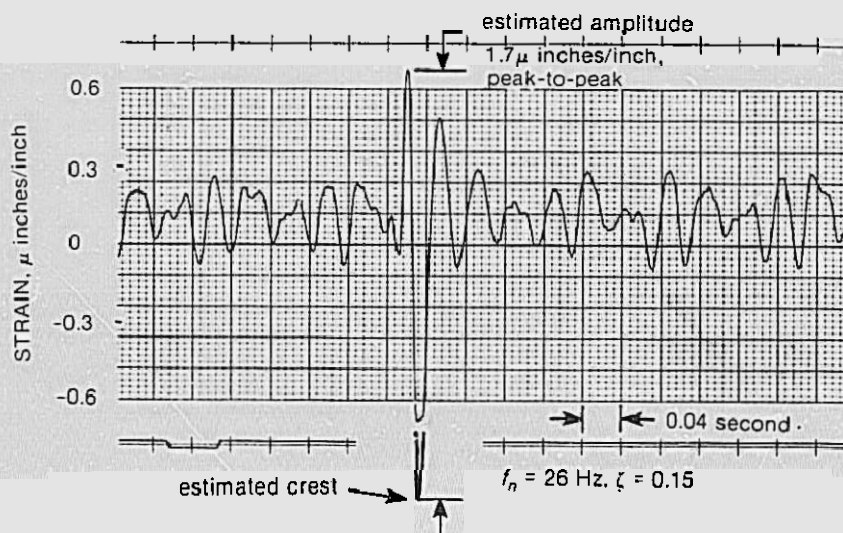


Figure 6.—Torsional oscillation of Unit 1 at Flatiron Powerplant — May 29, 1975

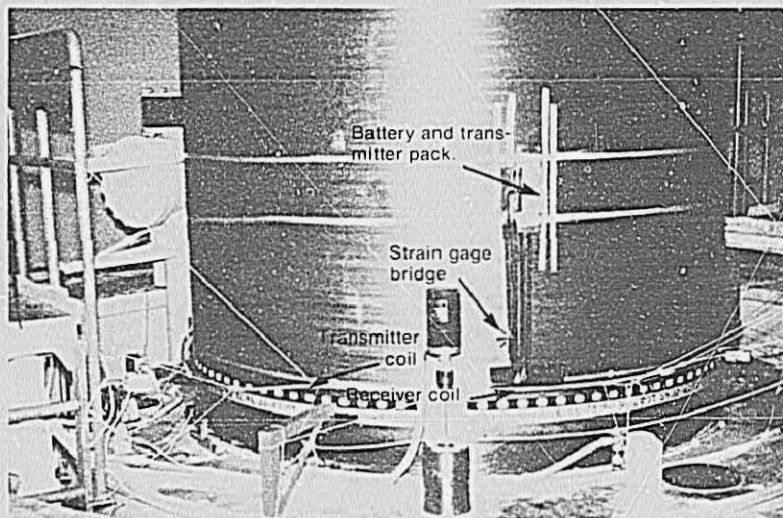
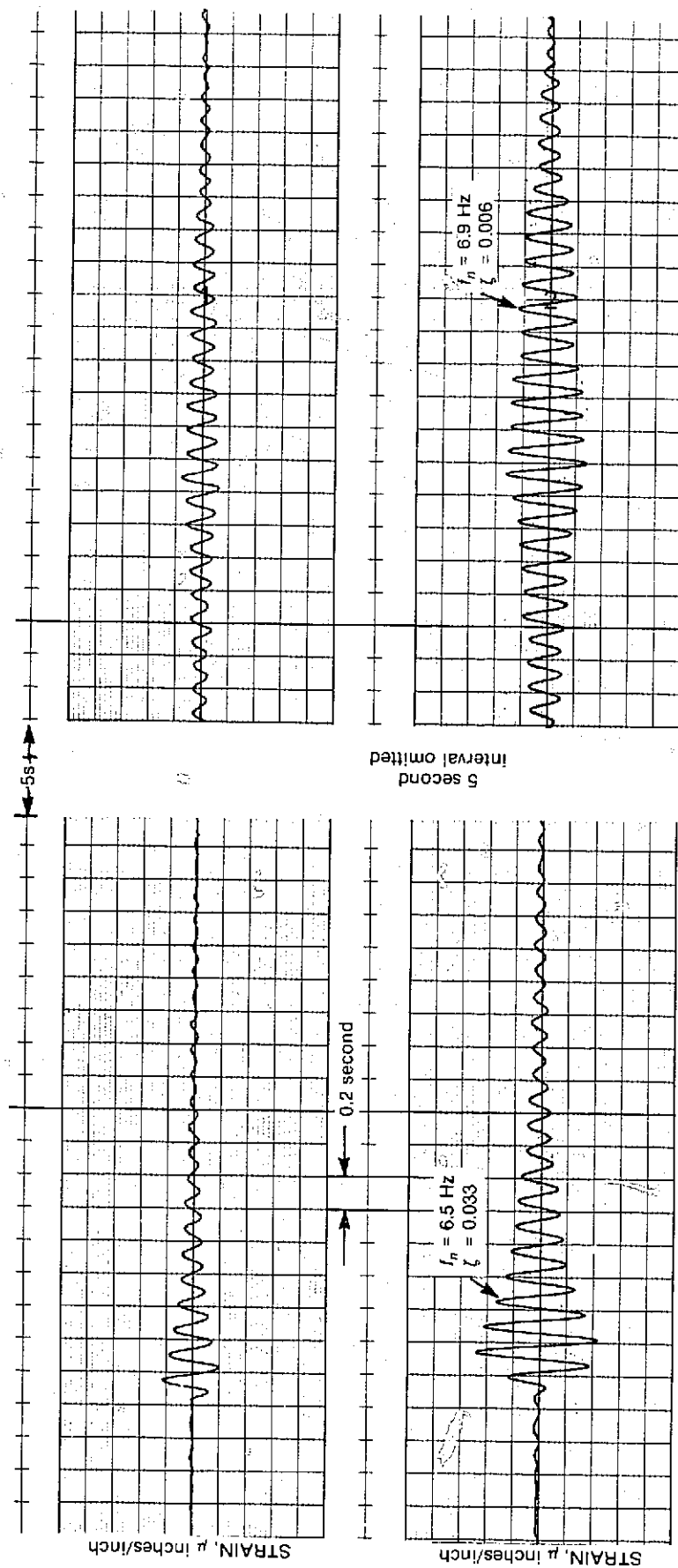


Figure 7.—Shaft torsional instrumentation system applied to Unit G19 at Grand Coulee — September 1975. Photo C801-D-79092



upper trace: unfiltered strain signal
lower trace: filtered strain signal from the fourth order bandpass filter tuned for: $5.5 \leq f \leq 7.5 \text{ Hz}$.

Figure 8.—Torsional oscillation excited by a 600-MW load rejection from Unit G19 at Grand Coulee — September 7, 1975.

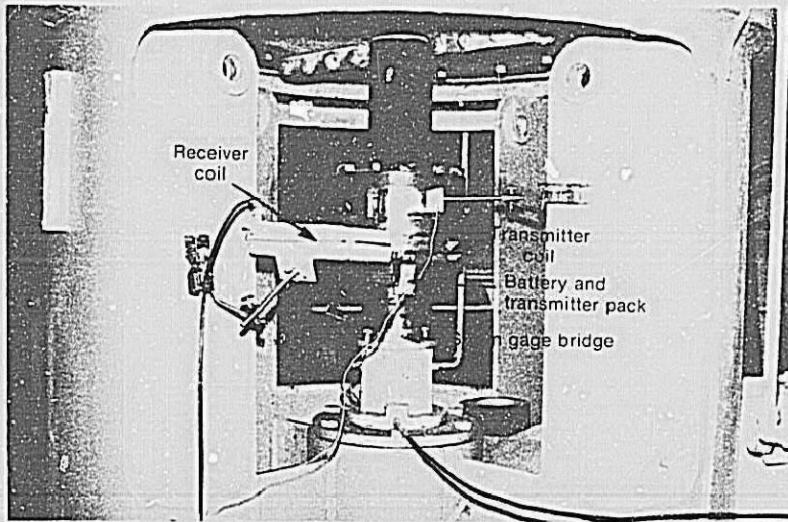


Figure 9.—Modified shaft torque instrumentation system applied to Unit 6 of Pumping Plant No. 1 of the Southern Nevada Water Project — January 1978. Photo C801-D-79093

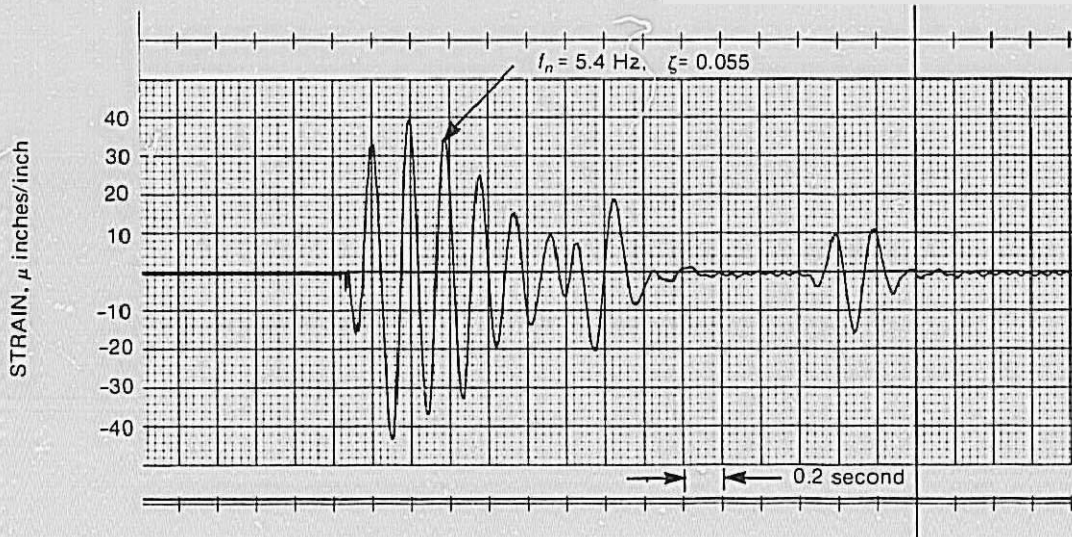


Figure 10.—Shaft torsional oscillation of Unit 6 of Southern Nevada Water Project, Pumping Plant No. 1 — January 13, 1978.

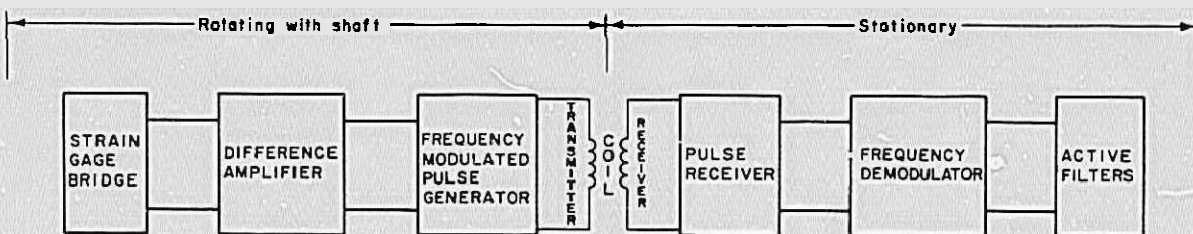
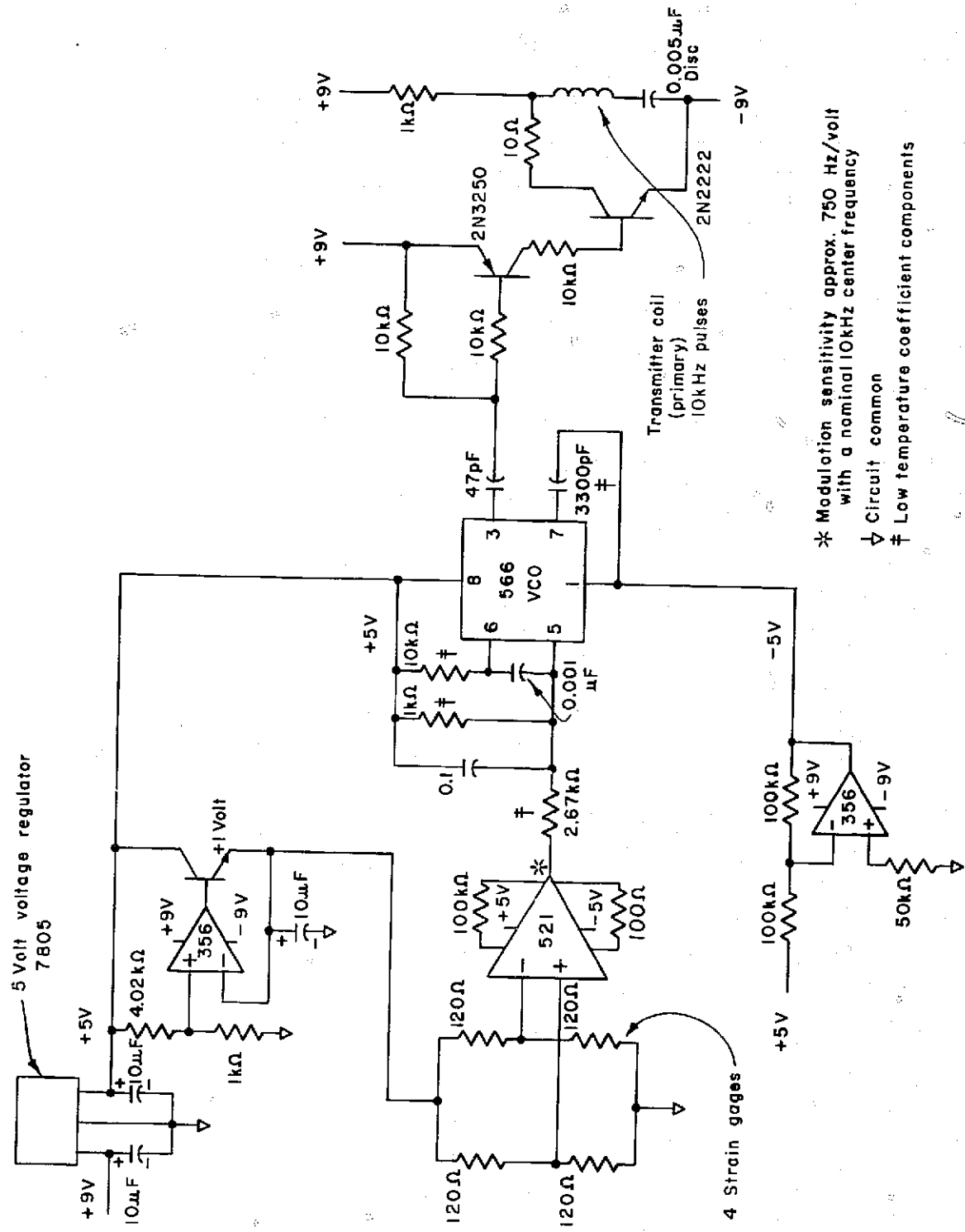
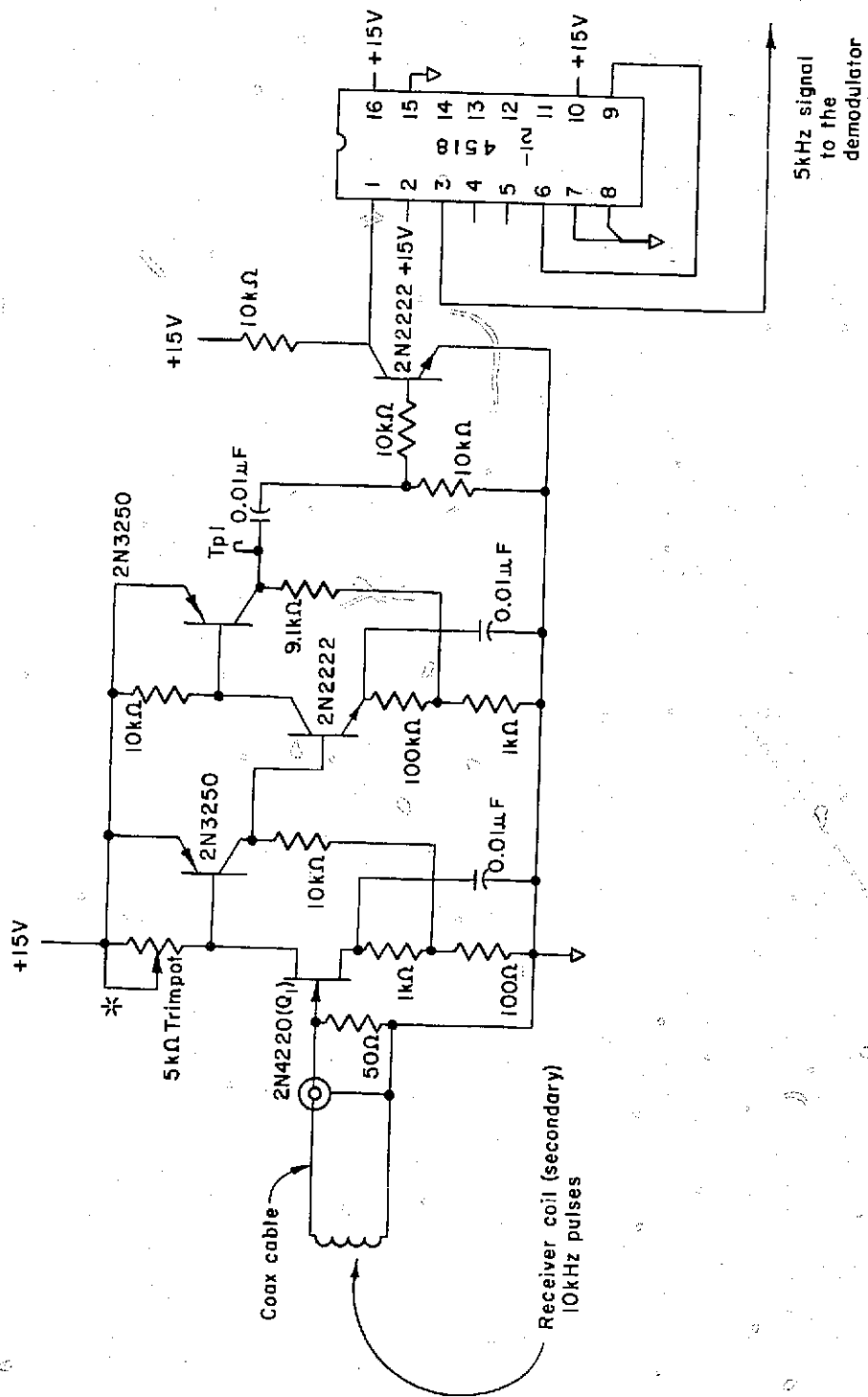


Figure 11.—Block diagram of the shaft torsional instrumentation system.



- * Modulation sensitivity approx. 750 Hz/volt with a nominal 10kHz center frequency
- ∇ Circuit common
- ‡ Low temperature coefficient components

Figure 12.—Torque sensor and frequency-modulated transmitter schematic.



- ▽ 5kHz signal to the demodulator
- ▽ Circuit common
- * Adjust trimpot for 2-5 volts d.c. at Tpl.

Figure 13.—Pulse receiver schematic.

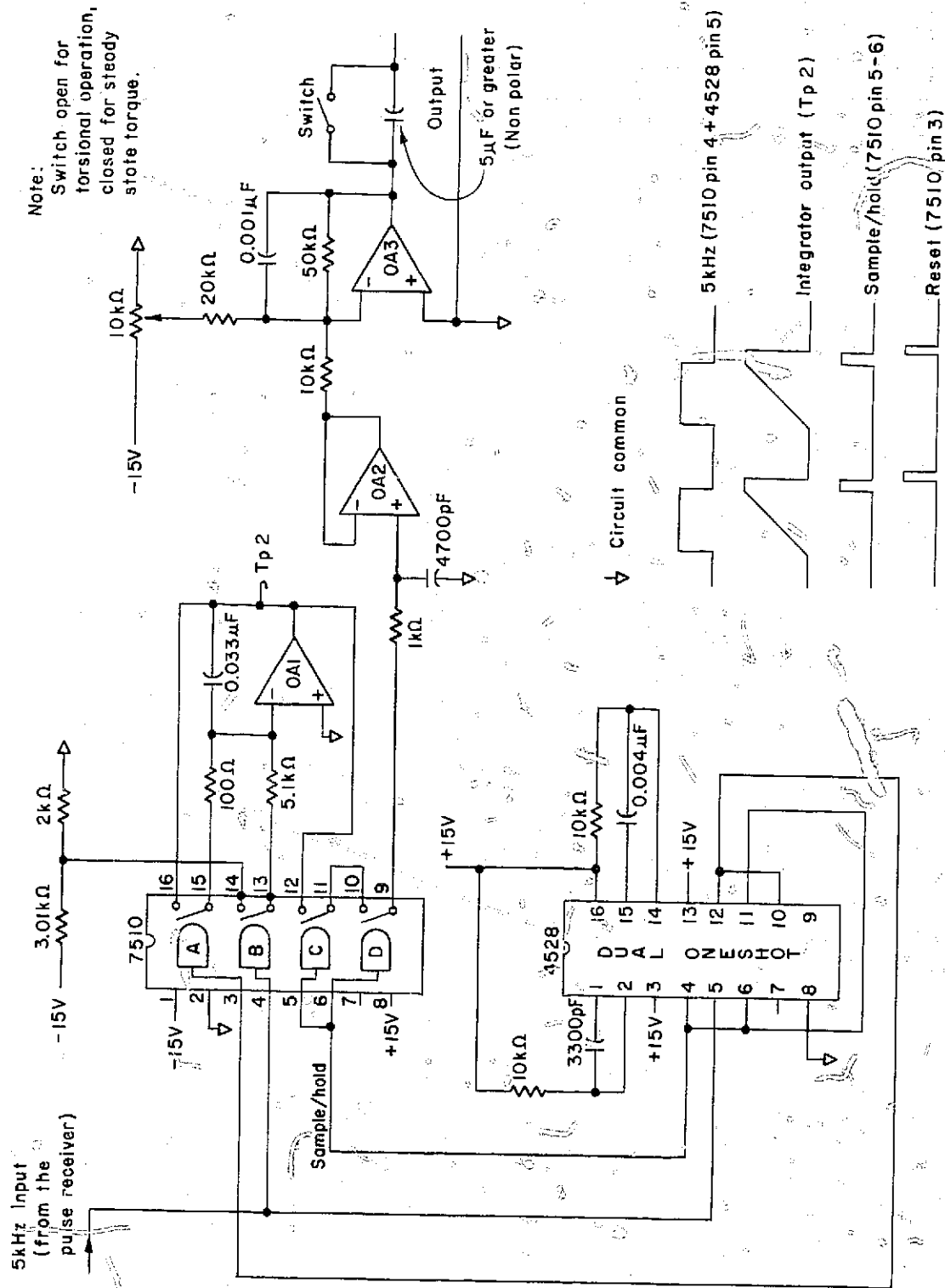


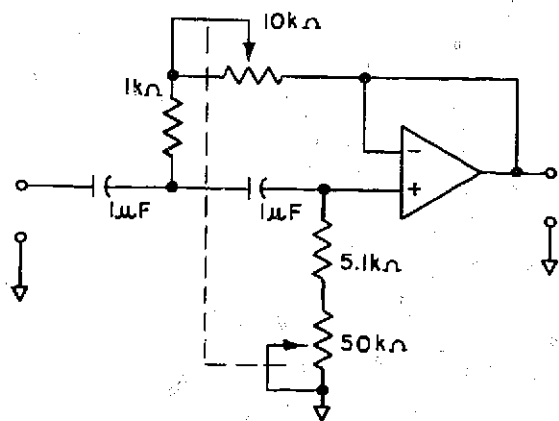
Figure 14. Demodulator (frequency transducer) schematic.

The final value at the output of the integrator is proportional to the time of one-half of the period of the 5-kHz square wave. Two other sections (C and D) of the analog switch together with operational amplifier OA2 comprise a sample-and-hold circuit which transfers the voltage from OA1 to output amplifier OA3. The remaining analog switch section (A) resets the integrator prior to the next positive excursion. Output amplifier OA3 provides d-c voltage proportional to strain.

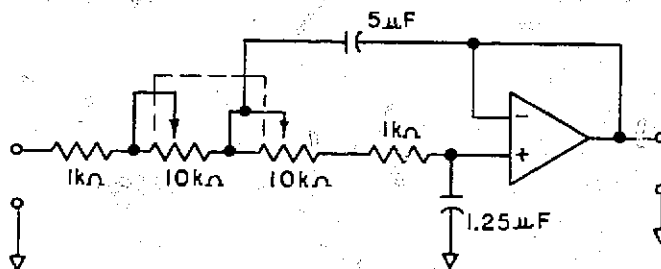
are used to process the torsional output signal before recording. The filter configuration easily permits selection of any or all of the filters by simple patching connections. Cascade connection of all of the available filter stages results in a fourth-order band-pass type of filter with adjustable low and high cut-off frequencies. The resulting filter exhibits good transient response (with little or no ringing or overshoot) and may be easily adjusted to the specific torsional mode sought.

Filter circuits.—

Two second-order high-pass and 2 second-order low-pass tunable active filters shown on figure 15



Corner frequency $\approx 3-35$ Hz
Second-order high pass filter



Corner frequency $\approx 5-60$ Hz
Second-order low pass filter

↓ Circuit common

Figure 15.— Schematic diagrams of the active filters.

APPENDIX A

APPENDIX A GENERAL SHAFT TORSIONAL DYNAMICS

Considering masses i and j and connecting shaft section S_{ij} on figure 1, the following equations may be written:

For the dynamics of the i th mass

$$\sum M_i = I_i \frac{d\omega_i}{dt} \quad (1)$$

expressing equation (1) in per unit

$$M_R \sum m_i = I_i \omega_R \frac{d\omega_i}{dt} \quad (2)$$

where M_R and ω_R are rated torque and rated angular velocity, respectively.

rearranging equation (2)

$$\sum m_i = \frac{I_i \omega_R}{M_R} \frac{d\omega_i}{dt} \quad (3)$$

From the definition of the mechanical starting time of the i th mass

$$T_{m_i} = \frac{n_R^2 (WR^2)_i}{1.6 \times 10^6 \text{hp}} = \frac{I_i \omega_R}{M_R} \text{ seconds}$$

therefore, equation (3) becomes

$$\sum m_i = T_{m_i} \frac{d\omega_i}{dt} \quad (3a)$$

or in Laplace notation

$$\sum m_i = T_{m_i} s \omega_i \quad (3b)$$

rearranging

$$\frac{1}{T_{m_i} s} \sum m_i = \omega_i \quad (4)$$

The torques applied to the i th rotating mass include the external torque m_i , the shaft reaction torques $m_{i-1,i}$ and $m_{i,i+1}$, and a damping torque $R_i \omega_i$.

Thus for mass 1:

$$\frac{1}{T_{m_1} s} (m_1 - m_{12} - R_1 \omega_1) = \omega_1 \quad (4a)$$

and for mass 2:

$$\frac{1}{T_{m_2} s} (m_2 + m_{12} - m_{23} - R_2 \omega_2) = \omega_2 \quad (4b)$$

etc.

For the dynamics of connecting shaft section S_{ij} , the internally transmitted torque is proportional to the angular torsional deflection $(\Theta_i - \Theta_j)$ of the shaft and the internal loss is proportional to differential shaft velocity, i.e.,

$$m_{ij} = K_{ij} (\Theta_i - \Theta_j) + D_{ij} (\omega_i - \omega_j) \quad (5)$$

But

$$\omega_i - \omega_j = \frac{d}{dt} (\Theta_i - \Theta_j) = s (\Theta_i - \Theta_j) \quad (6)$$

or

$$\Theta_i - \Theta_j = \frac{1}{s} (\omega_i - \omega_j) \quad (7)$$

so that equation (5) may be written

$$m_{ij} = \left[\frac{K_{ij}}{s} + D_{ij} \right] (\omega_i - \omega_j) \quad (8)$$

For example, the torque transmitted by shaft section S_{12} from mass 1 to mass 2 is given by:

$$m_{12} = \left[\frac{K_{12}}{s} + D_{12} \right] (\omega_1 - \omega_2) \quad (8a)$$

Equation 4a, 4b, and 8a which describe the dynamics of masses 1 and 2 and the connecting shaft section S_{12} are modelled in the block diagram of figure A1. Similar equations describing the motion of the other masses and shaft sections may be written and modelled as shown in figure A1 for the five element system of figure 1.

The dashed portions of figure A1 are included to show how the shaft torsional model may be integrated into stability studies or dynamic studies of the excitation or governing systems to assess the interaction of those systems with the shaft torsional modes.

DERIVED RELATIONS FOR SHAFT TORSIONALS

Shaft torsional oscillations of a two mass, single shaft system similar to that of figure 2 are characterized by simple harmonic motion for which the following equations may be shown to apply.

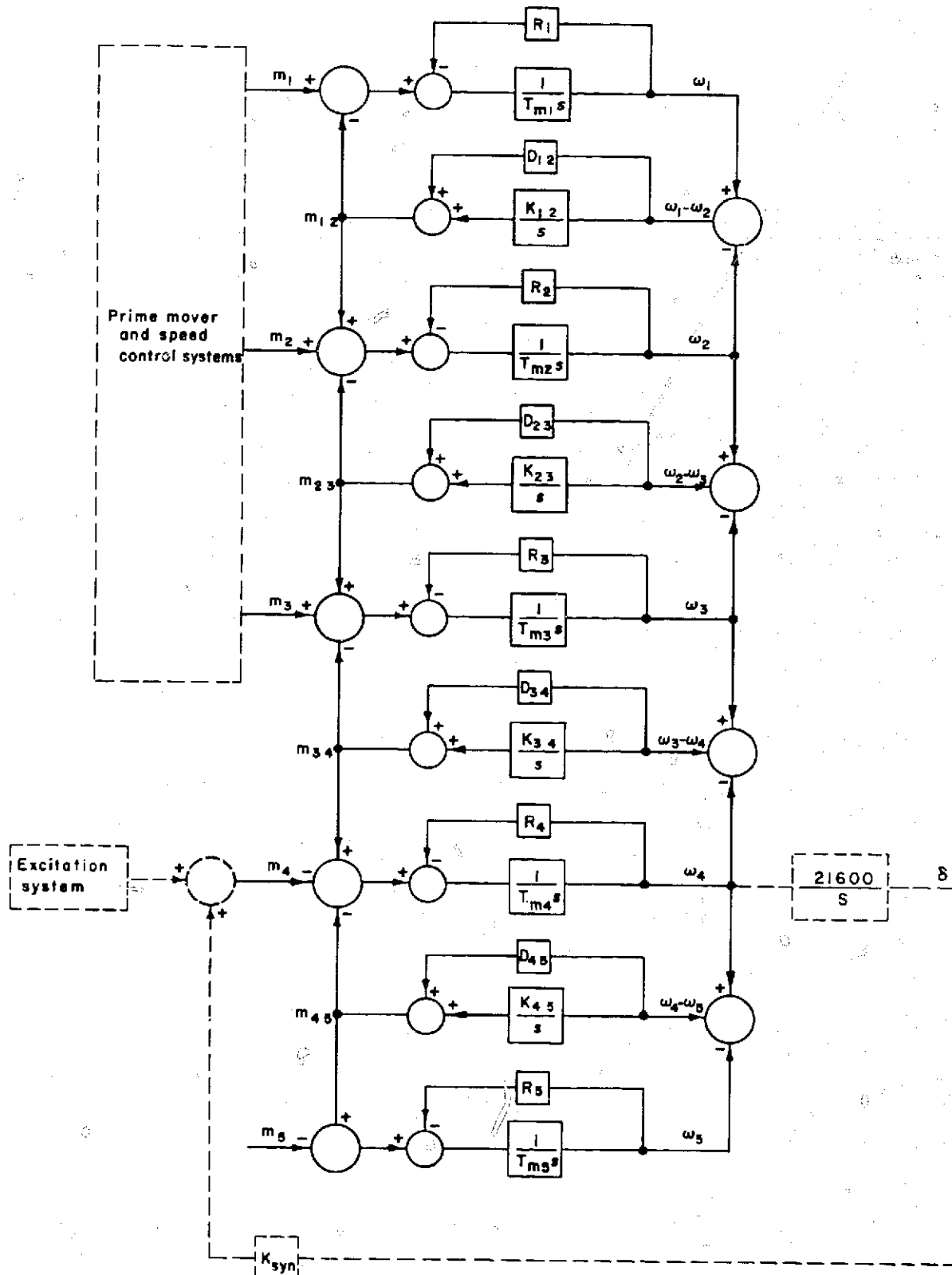


Figure A1.—Block diagram of the torsional system of figure 1.

Natural frequency f_n of the torsional oscillations:

$$f_n = \frac{1}{2\pi} \sqrt{\frac{6n_R K_{pu} (T_{m_t} + T_{m_g})}{T_{m_t} (T_{m_g})}}, \text{ Hz} \quad [6]$$

Angular amplitude $(\Theta_t - \Theta_g)_{peak}$ of the torsional oscillations resulting from a normalized torque (moment) m input through the generator:

$$\begin{aligned} (\Theta_t - \Theta_g)_{peak} &= \frac{T_{m_t} m}{K_{pu} (T_{m_t} + T_{m_g})}, \text{ degrees} \\ &= \frac{T_{m_t} m}{6n_R K_{pu} (T_{m_t} + T_{m_g})}, \text{ per unit} \quad [7] \end{aligned}$$

or

$$(\Theta_t - \Theta_g)_{peak} = \frac{m}{(2\pi f_n)^2 T_{m_g}}$$

per unit, where 1 per unit = $6n_R$ degrees

Assuming no damping, the shaft torsional oscillations may be represented by the following function of time:

$$\Theta_t - \Theta_g = (\Theta_t - \Theta_g)_{peak} \sin 2\pi f_n t, \text{ degrees} \quad [8]$$

Damping may be included by multiplying equation [8] by $e^{-\sigma t}$ where $\sigma = 2\pi f_n \zeta$ is the decrement factor.

From equation [8], the differential angular velocity $(\omega_t - \omega_g)$ may be obtained as

$$\begin{aligned} \omega_t - \omega_g &= \frac{d}{dt} (\Theta_t - \Theta_g) \\ &= 2\pi f_n (\Theta_t - \Theta_g)_{peak} \cos 2\pi f_n t \quad [9] \end{aligned}$$

Substituting from equations [6] and [7] and simplifying

$$\begin{aligned} \omega_t - \omega_g &= \frac{m}{2\pi f_n T_{m_g}} \cos 2\pi f_n t, \text{ per unit} \\ &= \frac{6n_R m}{2\pi f_n T_{m_g}} \cos 2\pi f_n t, \text{ degree/second} \end{aligned}$$

And the differential angular acceleration $(\alpha_t - \alpha_g)$ becomes

$$\begin{aligned} \alpha_t - \alpha_g &= \frac{d^2}{dt^2} (\Theta_t - \Theta_g) \\ &= -(2\pi f_n)^2 (\Theta_t - \Theta_g)_{peak} \sin 2\pi f_n t \quad [10] \end{aligned}$$

Substituting from equations [6] and [7] and simplifying:

$$\begin{aligned} \alpha_t - \alpha_g &= -\frac{6n_R m}{T_{m_g}} \sin 2\pi f_n t, \text{ degree/second}^2 \\ &= \frac{m}{T_{m_g}} \sin 2\pi f_n t, \text{ per unit/second} \end{aligned}$$

The tangential acceleration a at the surface of the shaft then may be found as

$$\begin{aligned} a &= \frac{D}{24} (\alpha_t - \alpha_g) \frac{\pi n_R}{30} \\ &= -\frac{\pi D n_R m}{720 T_{m_g}} \sin 2\pi f_n t, \text{ feet/second}^2 \\ &= -\frac{\pi D n_R m}{23 \cdot 184 T_{m_g}} \sin 2\pi f_n t, \text{ g's} \quad [11] \end{aligned}$$

The shaft surface deflection Δs per unit length due to the shaft torsional oscillations is determined by

$$\begin{aligned} \Delta s &= \frac{\pi}{0.36} \left(\frac{D}{L} \right) (\Theta_t - \Theta_g) \\ &= \frac{\pi}{0.36} \left(\frac{D}{L} \right) \frac{6n_R m}{(2\pi f_n)^2 T_{m_g}} \sin 2\pi f_n t, \text{ mils/inch} \quad [12] \end{aligned}$$

All the preceding relations written for a normalized torque (moment) m input through the generator may likewise be written for an input through the turbine by interchanging T_{m_t} with T_{m_g} throughout the procedure.

Also, all of the equations may be converted to the metric equivalents by replacing $6n_R$ and (D/L) with $180\omega_R$ and (d/l) , respectively.

APPENDIX B

APPENDIX B SIGNIFICANT SHAFT TORSIONAL PARAMETERS AND RELATIONS

CONSTANTS AND STEADY-STATE PARAMETERS

Rated moment M_R (torque)

$$M_R = 7.043 \times 10^6 P_R / n_R \text{ pound-feet} \dots \text{ U.S. customary} \quad [1]$$

$$M_R = 10^6 P_R / \omega_R \text{ newton-meters} \dots \text{ metric}$$

where

- n_R = rated speed in revolutions per minute
- P_R = generator rating in megawatts
- ω_R = rated angular velocity in radians per second

Shaft torsional spring constant K_{pm} in per unit torque per mechanical degree.

$$K_{pm} = \frac{\pi}{2160} \left(\frac{K \text{ in pound-inches/radian}}{M_R} \right) \text{ per unit/mechanical degree} \dots \text{ U.S.} \quad [2]$$

$$K_{pm} = \frac{\pi}{180} \left(\frac{K \text{ in newton-meters/radian}}{M_R} \right) \text{ per unit/mechanical degree} \dots \text{ metric}$$

The constant angular shaft deflection Θ_s at rated generator output is

$$\Theta_s = \frac{1}{K_{pm} \eta_g} \text{ degrees} \quad [3]$$

where

$$\eta_g = \text{generator efficiency}$$

The shaft surface deflection ΔS per unit length at rated generator output is

$$\Delta S = \frac{\pi \Theta_s}{0.36} \left(\frac{D}{L} \right) \text{ mils/inch} \dots \text{ U.S.} \quad [4]$$

or

$$\Delta S = \frac{\pi}{0.36 K_{pm} \eta_g} \left(\frac{D}{L} \right) \text{ mils/inch} \dots \text{ U.S.}$$

$$\Delta S = \frac{\pi \Theta_s}{0.36} \left(\frac{d}{l} \right) \frac{\text{millimeters}}{\text{meter}} \dots \text{ metric}$$

or

$$\Delta S = \frac{\pi}{0.36 K_{pm} \eta_g} \left(\frac{d}{l} \right) \frac{\text{millimeters}}{\text{meter}} \dots \text{ metric}$$

where

- D = shaft outside diameter in inches.
- d = shaft outside diameter in meters.
- L = overall shaft length in inches, and
- l = overall shaft length in meters.

Note: The overall shaft length is measured between the centroids of the turbine runner and generator rotor.

Mechanical starting time T_m of the turbine runner and/or generator rotor is

$$T_m = \frac{(n_R)^2 (WR^2)}{1.615 \times 10^6 \text{ hp}} = \frac{0.462 (n_R)^2 (WR^2) 10^{-9}}{P_R} \text{ seconds} \quad [5]$$

$$T_m = \frac{I (\omega_R)^2 10^{-5}}{P_R} \text{ seconds} \dots \text{ metric}$$

Note: The (WR^2) or I is that appropriate for the rotating mass for which T_m is being sought.